Advanced Composite Materials
Publication details, including instructions for authors and subscription information:
http://www.tandfonline.com/loi/tacm20

Experimental investigation of the effect of aging on perforated composite tubes under axial compressive loading

Shiva Eslami [a] , Ramadan A. Esmaeel [a] & Farid Taheri [a]

[a] Department of Civil and Resource Engineering , Dalhousie University , 1360 Barrington Street, Halifax , Nova Scotia , Canada , B3J 1Z1

Published online: 02 Apr 2013.

To cite this article: Shiva Eslami , Ramadan A. Esmaeel & Farid Taheri (2013) Experimental investigation of the effect of aging on perforated composite tubes under axial compressive loading, Advanced Composite Materials, 22:3, 151-164, DOI: 10.1080/09243046.2013.782806

To link to this article: http://dx.doi.org/10.1080/09243046.2013.782806

Advanced Composite Materials, 2013
Vol. 22, No. 3, 151–164, http://dx.doi.org/10.1080/09243046.2013.782806

Taylor & Francis
Taylor & Francis Group

Experimental investigation of the effect of aging on perforated composite tubes under axial compressive loading

Shiva Eslami, Ramadan A. Esmaeel[1] and Farid Taheri*

Department of Civil and Resource Engineering, Dalhousie University, 1360 Barrington Street, Halifax, Nova Scotia, Canada, B3J 1Z1

(*Received 20 June 2012; accepted 4 March 2013*)

The use of fiber-reinforced polymer (FRP) composite materials in various applications such as aerospace, automotive, sport equipment, and oil and gas industries has been growing in a steady rate in recent years. The potential use of perforated FRP tubes (pipes) in oil and gas industry-related applications can become significantly greater, provided that the influence of the harsh environmental conditions specific to the industry could be tolerated by the materials used to form such tubes, with minimal degradation to system's mechanical and physical properties. Unfortunately, there is not adequate database and information in the literature in regards to the long-term response of perforated FRP tubes. The purpose of this study is therefore to investigate whether FRP could be confidently used in structural applications that are primarily subjected to compressive loading and exposed to harsh environments, without significant deterioration of their physical and mechanical properties. For that, three sets of perforated glass fiber-reinforced plastic (GFRP) pipes were fabricated and subjected to accelerated aging conditions in an acid. Subsequently, the pipes were tested to failure under an axially applied compressive load. Results showed a considerable decrease in the load carrying capacity and axial stiffness of perforated pipes having certain D/t ratios, as a result of the aging.

Keywords: axial loading; laminated cylindrical tubes; perforation; experimental investigation

1. Brief review of the relevant research

The use of fiber-reinforced polymer (FRP) materials to fabricate wastewater pipes has gained popularity in recent years as several wastewater treatment plants are currently replacing their traditional steel with pipes made of FRP. However, the presence of harsh environments can accentuate the corrosion process in FRP pipes. Due to the chemical nature of the polymeric matrix used in FRP, the loss in the mechanical properties can be attributed to the resin plasticization, and more importantly, to the degradation of the fiber/matrix interface bond.[1] The rate of degradation would be a strong function of the surrounding corrosive environment temperature. For instance, most epoxy matrices are recommended for use in environments with temperatures below 60 °C, as the thermally induced degradation is usually initiated at 70 °C.[2] Long-term exposure of FRP to corrosive environments at elevated temperatures has been shown to also strongly affect the fiber strength.[3]

*Corresponding author. Email: farid.taheri@dal.ca
[1]On leave from: Faculty of Engineering, Fayoum University, Fayoum, Egypt.

Startsev et al. [4] showed that the exposure of polymer composites to climatic aging would cause the through-the-thickness mechanical properties across the thickness to significantly degrade. Tsotsis et al. [5] observed that FRP specimens' aging process was significantly accelerated when the material was subjected to large pressure magnitudes (especially in those with $[\pm 45^{\circ}]_{2s}$ layup, which were subjected to a tensile load). Boukhoulda et al. [6] subjected artificially aged E-glass/polyester composite plates to impact forces by means of a drop-mass. They reported the non-Fickian and Langmuir-type characteristics of the moisture absorption kinetics of the plate specimens.

Using the fracture mirror measurements on the broken ends of the fibers, Liao et al. [7] provided clear evidence that the fiber strength of the pultruded glass fiber-reinforced vinyl-ester matrix composite coupons was decreased due to aging of the composite in water. Abdel-Magid et al. [8] studied aging of E-glass/epoxy composite specimens by conditioning their FRP specimens in wet environment under an applied mechanical loading. Their results revealed that a noticeable loss in the mechanical properties (modulus and strength) took place as a result of the combined effects of loading, moisture, and temperature. Bagherpour et al. [9] examined the effects of concentrated HCl acid on the mechanical response of a fiber-glass polyester composite. Their scanning electron microscope (SEM) micrographs evidenced a considerable strength reduction due to the loss of the fiber/matrix interfacial bond.

The degradation of the mechanical properties of glass/epoxy tubular specimens as a result of environmental effects has also been studied experimentally by Ellyin and Maser [10]. They immersed their filament wound specimens in distilled hot water for four months and noticed that the swelled matrix negatively impacted the functional failure of the specimens. Moreover, the plasticization that occurred in the matrix reduced its stiffness considerably and also reduced the cohesion of the fiber/matrix interface, thus giving a greater chance for fiber pull-out. Guedes et al. [11] studied the effect of moisture absorption on the creep response of glass-fiber/thermosetting-matrix composite pipes. As a conclusion, they stated that the use of the power law relationship could provide a good prediction of the long-term response of such pipes. Yao and Ziegmann [12] performed an experimental investigation on the effect of moisture and temperature aging on the mechanical performance of glass/epoxy composite pipes under three-point bending loading conditions. They suggested that moisture would exhibit similar effect on aging as temperature would. Almeida et al. [13] verified the Fick model's applicability for describing the water absorption response of glass/vinyl-ester composite pipes.

In this paper, the stability response of perforated E-glass/epoxy pipes, having been aged in an acidic environment, has been investigated experimentally. The response of the aged pipes was then compared to that of their healthy (un-aged) counterparts.

2. Experimental investigation

In this study, full-scale composite tube specimens were fabricated and tested in both healthy and aged states. Detailed description of specimen preparation, ageing conditions, and experimental procedure will be described in the following sections.

2.1. Fabrication and conditioning of glass fiber-reinforced plastic cylindrical specimens

All glass fiber-reinforced plastic (GFRP) pipes considered in this study were fabricated by wrapping two or three layers of a stitched fabric having a typical ply sequence of [45°/−45°/90°] (angles are with respect to the longitudinal axis of the pipes). To facilitate the release of the specimens from mandrel, a temperature-resistant mold-release agent was applied to the outer surface of the mandrel. The alignment of the final pipe specimens was checked using a

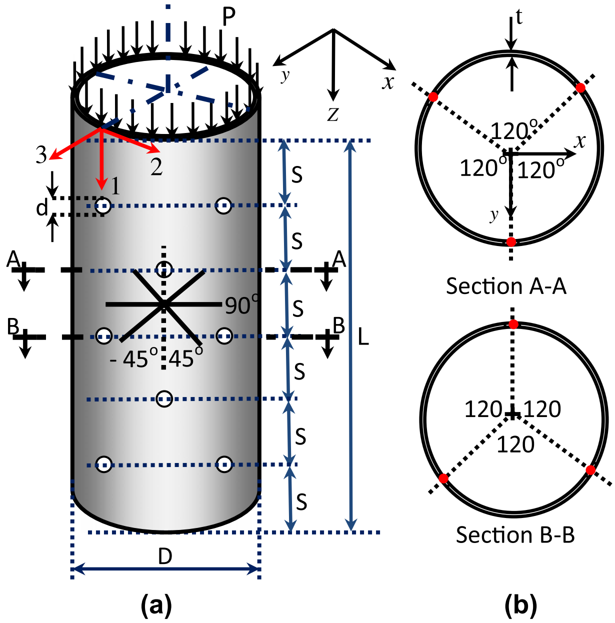

Figure 1. Perforated tube: (a) tube geometry, (b) cross sections showing perforation arrangements.

dial gage having a resolution of 0.01 mm, while the thickness of the cured pipes was measured using a digital micrometer with 0.01 mm accuracy. All specimens were then carefully cut to the specified length using a diamond-coated saw, ensuring that their edges were parallel, and orthogonal to the pipe axial axis to facilitate a uniformly distributed load during testing. A total of 36 pipe specimens were fabricated, half of which were professionally perforated using a high-speed milling machine. The perforation pattern and the details of the geometrical features of the test specimens are clearly shown in Figure 1. The total length of each pipe specimen was $L = 300$ mm with a distance of $S = 50$ mm between the rows of perforations (see Figure 1). The 36 specimens were divided into two main categories: perforated and non-perforated. Each category was divided into three subcategories according to specimen's diameter to thickness ratio (i.e. $D/t = 48.8$, 71.5, and 27.5, respectively). More information on specimens' identification/classification code and the dimensions are provided in Table 1.

Three out of six specimens per subcategory were submerged in a 15% diluted sulphuric acid and placed in a temperature-controlled chamber at 60 °C until saturation. The acid, its concentration, and temperature were chosen to simulate the harsh chemical environment typically experienced by liners in directional oil wells. The purpose of the elevated temperature was to simulate the typical environment found in most directional oil wells, which expedites the aging process.

Table 1. Test specimens specification.

Code	Inner diameter (mm)	Wall thickness (mm)	Lay up	Condition
AI	107.3	2.2	$[\pm45^o/90^o]_3$	Intact
AP		2.2	$[\pm45^o/90^o]_3$	Perforated
BI	107.3	1.5	$[\pm45^o/90^o]_2$	Intact
BP		1.5	$[\pm45^o/90^o]_2$	Perforated
CI	60.4	2.2	$[\pm45^o/90^o]_3$	Intact
CP		2.2	$[\pm45^o/90^o]_3$	Perforated

2.2. Test equipment and procedure

Specially designed grips were fabricated to hold the test specimen in the loading machine; this fixture is composed of two circular end plates having a 10 mm deep groove. The grooves were basically used to prevent the thin-walled specimen from slipping during the application of the compressive load. An INSTRON servo-hydraulic universal testing machine controlled with 8600+ electronics was used for testing the specimens. The grips and test setup are shown in Figure 2. To maintain a concentric axial load throughout the experiment, the upper circular plate was composed of two thick plates separated by a steel ball to prevent any misalignment due to the applied axial load. The specimens were loaded axially at a rate of 0.5 mm/min, and the applied load was measured using a 250 kN load cell, while the ends shortening was established through the actuator's crosshead movement, recorded by the electronics. For each specimen group, at least one specimen was instrumented with a set of strain gages, mounted at the mid height of the specimen, on the two opposing faces. The main purpose of these gages was to ensure that the axial load was applied in a concentric fashion and that the specimens were experiencing a uniformly distributed axial strain.

The aged specimens were tested immediately after having been taken out of the environmental chamber. Specimens were covered with plastic wrap to avoid the evaporation of the acid from the specimen during the transportation of the specimens from the chamber to the testing lab. For specimens receiving strain gages, a small window was cut off the plastic wrap to allow for the surface preparation and installation of the gages. Since the aged specimens were submerged in the sulphuric acid and were fully saturated by the acid, their surfaces needed to be neutralized using a sodium hydroxide solution before the strain gages could be installed.

The strain gages' data were captured through a data acquisition system with an analog input module (NI-9215, in cDAQ-9172 Compact Chassis, manufactured by the National Instruments Inc., Austin, Texas). The sampling frequency was kept at 20.0 kHz during all experiments.

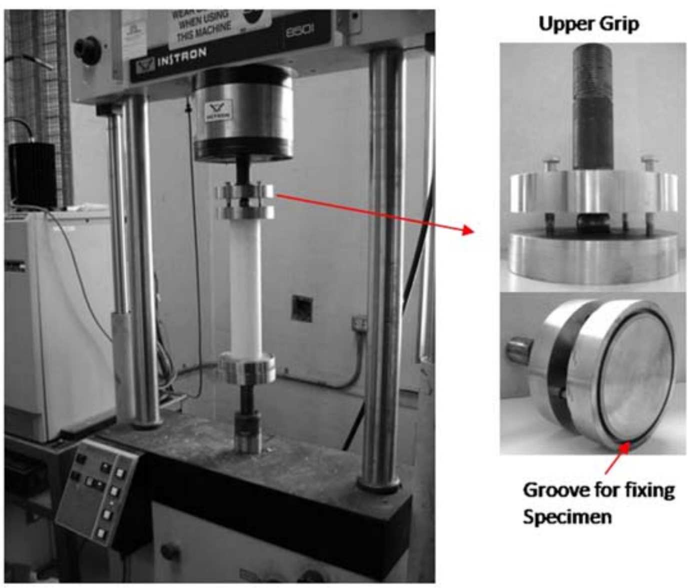

Figure 2. Buckling test facility.

3. Results and discussion

As stated, the foremost objective of this research work is to investigate the aging effects on the axial compressive load carrying capacity and stability response of the perforated GFRP pipes conditioned in an acidic environment. Typical failure patterns observed in the un-aged and aged specimens are illustrated in Figure 3. The visual inspection of the pipes, immediately after the specimens were taken out of the chamber, clearly evidenced a considerable loss of resin in the aged specimens. It was also evident that the material was fully saturated by the acid; as a result, the saturated specimens' wall-thickness was increased by approximately 10% compared to that of un-aged (virgin) counterparts.

3.1. Influence of acidic and elevated environment on the material

Prior to discussion of the test results, it would be prudent to briefly review the diffusion mechanism of liquids into composites. In polymer composites, the diffusion process could be modeled using Fick's solution, described by the following [13]:

$$\frac{M_{\%}}{M_{\mathrm{m}}} = 1 - \frac{8}{\pi^2}\sum_{n=0}^{\infty}\frac{1}{(2n+1)^2}\exp[-D_{\mathrm{c}}(2n+1)^2\pi^2 T/h^2] \tag{1a}$$

Which can be simplified and represented by

$$\frac{M_{\%}}{M_{\mathrm{m}}} = \tanh\left[\frac{4}{h}\sqrt{\left(\frac{D_c T}{\pi}\right)}\right] \tag{1b}$$

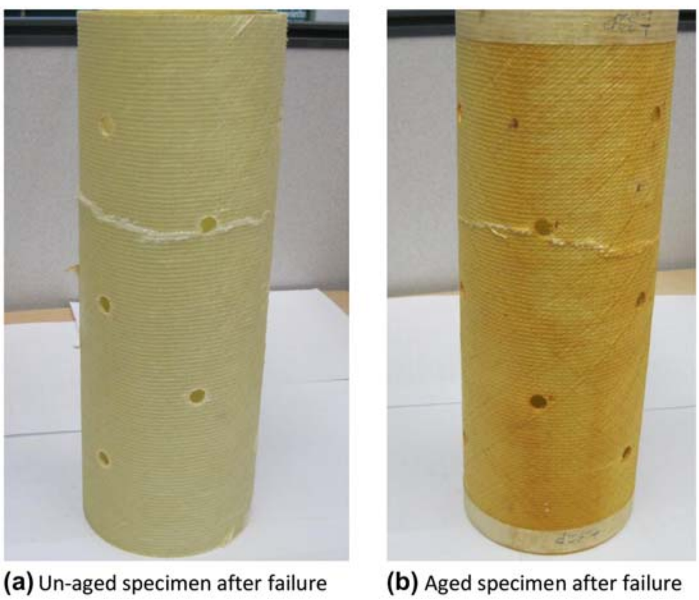

Figure 3. Typical failure patterns.

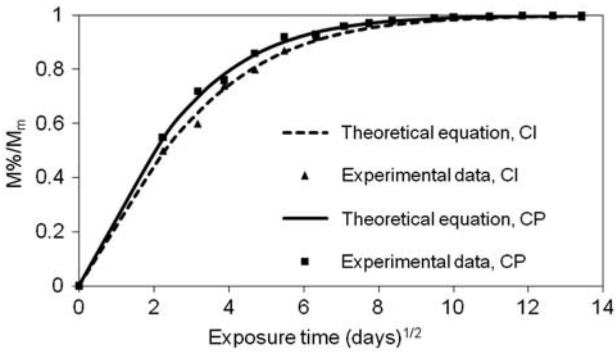

Figure 4. Variation of mass absorption as a function of time for pipe with $D/t = 27.5$ aged in 15% sulphuric acid at 60 °C.

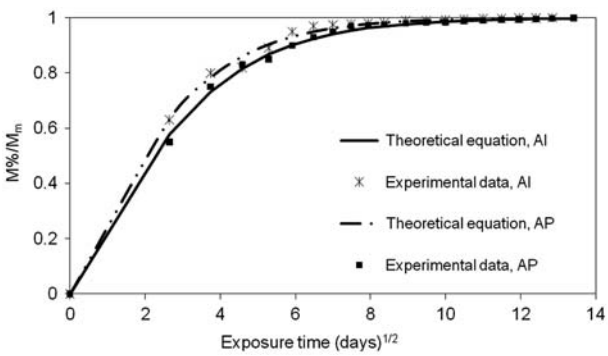

Figure 5. Variation of mass absorption as a function of time for pipe with $D/t = 48.8$ aged in 15% sulphuric acid at 60 °C.

In the above equations, $M\%$ is the percent liquid (here, acid) absorbed at time T, and M_m is the maximum liquid contents, respectively, D_c is the diffusion coefficient and h is specimen's thickness.

The mass change rate in the specimens can be calculated by:

$$M_t = \frac{m - m_0}{m_0} 100\% \quad (2)$$

where m_0, m, and M_t are the initial mass, the mass content at time T, and the absorbed mass percent at time T, respectively.

The weight change rate curves versus the square root of exposure time in aged specimens made from the materials used to fabricate the pipes are illustrated in Figures 4–6 for various composite thicknesses, diameters, and perforation conditions. In these figures, the solid symbols illustrate the experimental test results and the solid line reflects the results obtained using the theoretical model (i.e. Equation 1-b). Comparison of the absorption curves at different D/t ratio indicates that an increase in the ratio would increase the absorption rate; furthermore, it also implies that the perforations would facilitate further diffusion, hence accelerating the absorption rate.

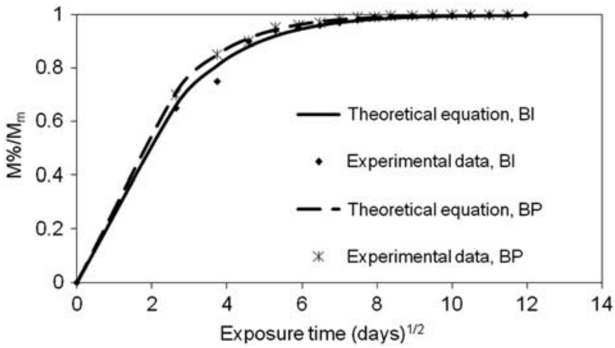

Figure 6. Variation of mass absorption as a function of time for pipe with $D/t = 71.5$ aged in 15% sulphuric acid at 60 °C.

3.2. *Influence of acidic and elevated environment on the load bearing capacity of the pipes*

Figure 7 shows the axial load versus end-shortening curves of typical virgin and aged non-perforated (intact) and perforated tubes with D/t ratio of 48.8. A considerable decrease in both the load carrying capacity and axial stiffness of the pipe is evident. The load carrying capacity and axial stiffness of each group of specimens investigated in this study are reported in Table 2, based the specimen codes identified in Table 1. It can be seen from the results presented in this table that the axial stiffness of the aged pipes decreased by a maximum of 57%, facilitating maximum end shortening of 46%, while the critical load was decreased by a maximum of 48%. Interestingly, the relative decrease in the ultimate strength of perforated pipes after aging was lower than that of the non-perforated aged pipes (by approximately 28%). Moreover, the aged non-perforated pipes exhibited greater end shortening than the perforated aged pipes; nevertheless, the overall axial stiffness of the aged perforated and non-perforated pipes was similar. As also seen, the responses of the aged specimens (for both virgin and perforated pipes) are somewhat nonlinear, evidencing the plasticization of the resin. The comparison of the axial and hoop

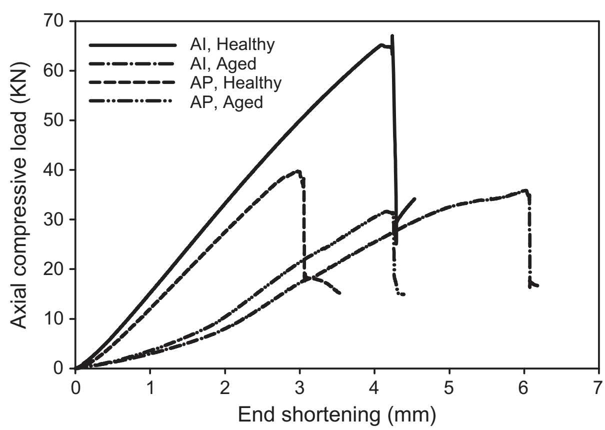

Figure 7. Experimental load versus end-shortening curves (AI and AP, $D/t = 48.8$).

Table 2. Experimental results of buckling tests.

D/t	Code	Axial stiffness (N/mm)	Critical load (N) Healthy pipes	End-shortening (mm)	Axial stiffness (N/mm)	Critical load (N) Aged pipes	End-shortening (mm)
48.8	AI	18,071	66,295	4.15	7692 (57%)[a]	34,128 (48%)	6.07 (46%)
	AP	15,794	43,122	3.08	9985 (37%)	31,050 (28%)	4.24 (38%)
71.5	BI	9622	28,069	3.55	8750 (9%)	26,588 (5%)	4.26 (20%)
	BP	7849	18,020	2.63	4800 (38%)	15,035 (17%)	4.13 (57%)
27.5	CI	10,729	36,276	4.01	10,100 (6%)	35,384 (%)	4.39 (9%)
	CP	9858	27,563	3.31	9850 (0%)	25,213 (%)	3.57 (8%)

[a]The tabulated percentiles (in absolute sense) reflect the change in the parameters calculated with respect to the corresponding parameters measured in the healthy specimens.

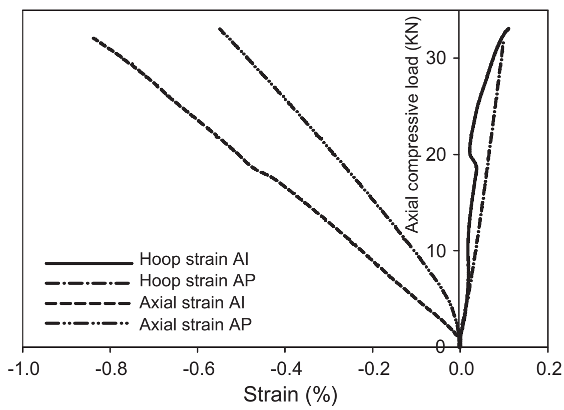

Figure 8. Hoop and axial strains for non-perforated and perforated pipes (AI and AP, $D/t=48.8$).

strains of ($D/t=48.8$) group aged pipes is shown in Figure 8. As seen, the non-perforated pipes experience larger axial strain than the perforated pipes.

To further investigate the effect of aging of perforated pipes, the results of the second group of specimens ($D/t=71.5$) are shown in Figures 9 and 10. It should be noted that this set of pipes has the same inner diameter as the first group, but their wall-thickness is thinner (2/3 of the previous group). It can be inferred from Figure 9 that the steady axial stiffness (i.e. the slope of the major linear portion of the load-deformation curve) is only 14% lower that of the healthy pipes as a result of aging. However, for the perforated pipes, this ratio jumped to almost 39% as shown in Figure 9. This decrease in the axial stiffness can be attributed to the fact that the existence of perforations increased the acid absorption areas and hence decreasing the overall stiffness of the aged pipes. In the case of the non-perforated pipes, there was virtually no change in the axial load carrying capacity of the virgin and aged pipes almost no change in the load carrying capacity of the non-perforated pipes after aging, however, there was a noticeable decrease in the maximum sustained load

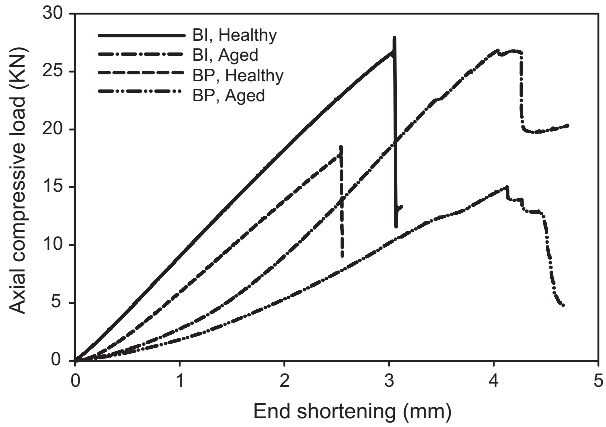

Figure 9. Experimental load vs. end-shortening curves (BI and BP, $D/t = 71.5$).

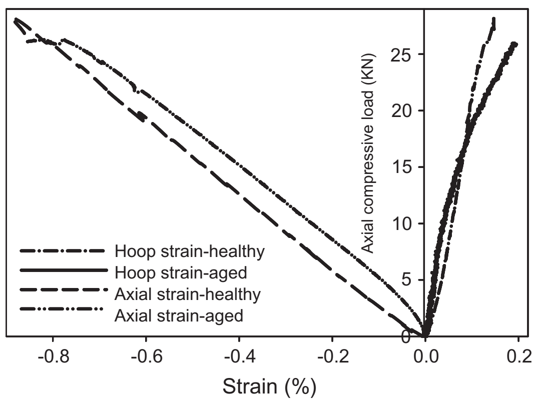

Figure 10. Hoop and axial strains for non-perforated pipes in both healthy and aged states (BI, $D/t = 71.5$).

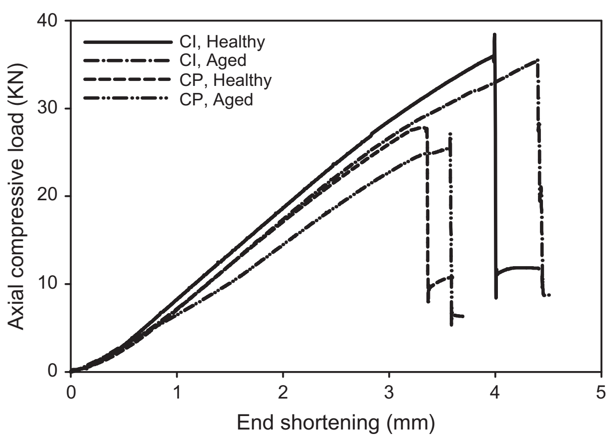

Figure 11. Experimental load vs. end-shortening curves (CI and CP, $D/t = 27.5$).

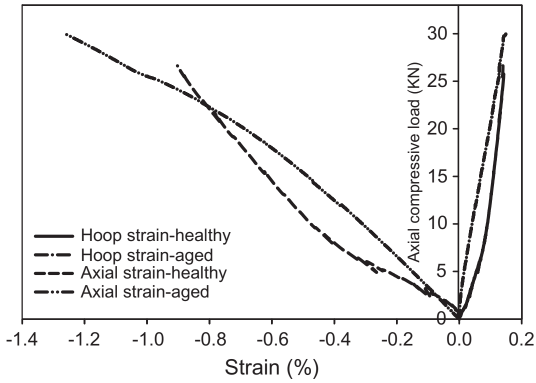

Figure 12. Hoop and axial strains for non-perforated pipes in both healthy and aged states (CI, $D/t=27.5$).

by the perforated pipes of the same group. All the aged pipes in both categories exhibited a noticeably larger deformation before reaching the ultimate failure load. In fact, in some cases, the aged pipes deformed more than one and half times of that of the virgin counterpart. The results obtained from the strain gages placed at the mid-height of both healthy and aged pipes are shown in Figure 10. The nonlinear variation of the strain as a function of the applied load of the aged specimens, which is in concert to the response of aged specimens depicted in Figure 9, further confirms the resin plasticization phenomenon as a result of aging in the acidic solution.

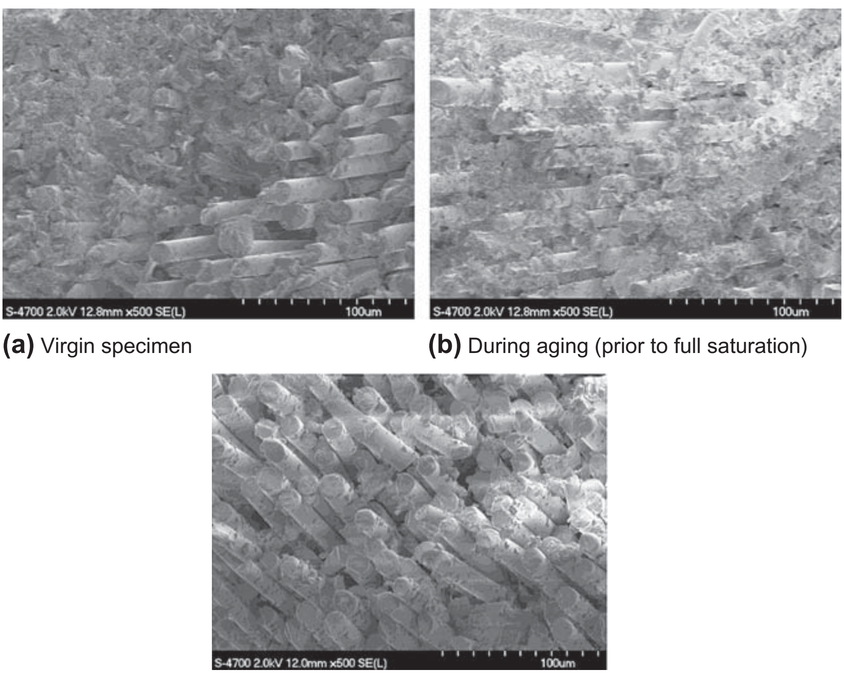

(a) Virgin specimen **(b)** During aging (prior to full saturation)

(c) Aged specimen (at fully saturated stage)

Figure 13. Comparison of the typical failure surfaces of the virgin and aged specimens.

The third group of specimens, comprised of a set of a smaller diameter pipes (i.e. with $D/t = 27.5$), when compared to the first two groups ($D/t = 48.8$ and 71.5), but had the same thickness as those in Group 1. Figures 11 and 12 present third group's results. There was no considerable change in either the axial stiffness or the load carrying capacity as a result of the aging in comparison to the appreciable changes noted in the test results of the first two groups. The noted response is believed to be due to the comparatively limited surface areas for the acid to wick into the composite, since in comparison, both the surface area of the small diameter pipes and the total cross-section area of the perforations are lesser when compared to the first case. This hypothesis is further supported by noticing the slightly lower ultimate capacity exhibited by the perforated pipes of this group in comparison to the non-perforated pipes; there is indeed a marginally larger cross-section area for the acid to wick into the composite in the case of the perforated pipes compared to the non-perforated pipes, though the area is not as appreciable as that in Group 1. To complete the comparison, the strain gages' results of a representative pipes in this group are also presented in Figure 12.

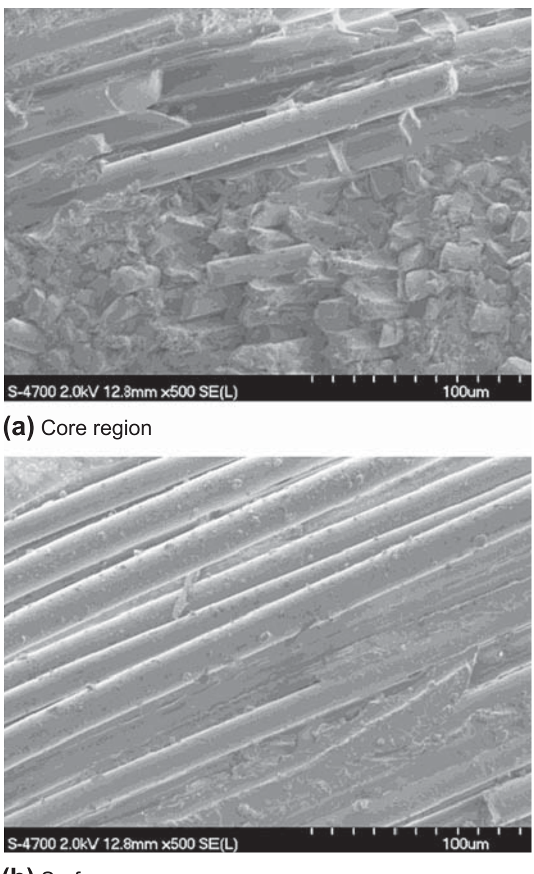

(a) Core region

(b) Surface

Figure 14. SEM images (through-the-thickness) of the smallest D/t saturated pipe.

3.3. *Influence of acidic and elevated environment on the microstructure of the pipes*

The influence of diffusion of the acidic solution on the perforated/non-perforated composite pipes and its effect on their micro-structures was also examined with the aid of SEM images.

Figure 13 shows the SEM pictures of the glass/epoxy pipes before, during, and after acid immersion. Good adhesion between the fibers and matrix is observed in the images of the pipes' material that was not exposed to acidic aging process. However, after having the material exposed to the corrosive medium at elevated temperature, its interfaces became weakened, leading to significantly reduced volume of resin surrounding the fibers.

Further examination of the failed cross-section of the thicker-walled pipes clearly revealed that the corrosive outcome was more sever at specimens' surface and gradually became milder as specimens' interior core region is considered (see Figure 14). When the outer layer resin and fibers are degraded due to exposure to acid, the stresses are shifted towards the fibers at the core region, thus leading to a decrease in the load bearing capacity of the fibers and initiation of cracks. The combination of the tangential and radial stresses facilitates creation of the initial crack and the subsequent propagation in a helical pattern.[14] The evidences of such helical crack growth on the fibers can be seen in Figure 15.

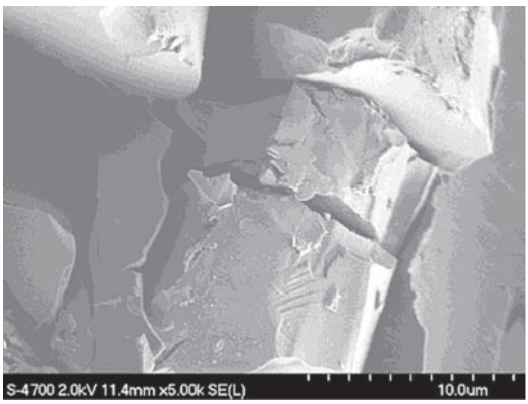

(a) Transverse cracks through the fiber after aging in 15% sulphuric acid

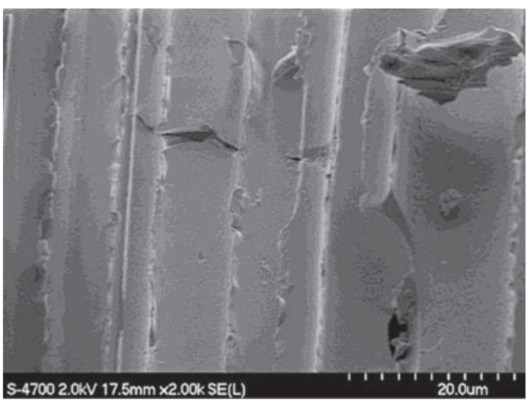

(b) transverse cracks through fibers and the resin after 15% sulphuric acid

Figure 15. Transverse crack pattern through fibers.

4. Conclusions

An experimental investigation was conducted in this study to assess the influence of aging of perforated glass/epoxy composite pipes within a combined harsh acidic and thermal environment, mimicking the ambient environment of most directional oil wells. The concluding remarks of this study can be summarized as follows:

- The epoxy resin used to fabricate the FRP specimens was significantly affected and dissolved at the end of the aging process.
- The remaining resin experienced the plasticization phenomenon, thereby rendering a nonlinear deformation. As a result, the aged pipes exhibited larger axial deformation prior to the final failure.
- Another major effect that can explain the loss in the load carrying capacity of the test specimens due to aging was the considerable loss of fiber/matrix interface adhesion.
- Pipes with larger D/t ratios showed more degradation in the mechanical properties and experienced more sever loss in their load carrying capacity as a result of aging in the combined acidic/thermal environment. This is believed to be due to the larger area available to the acid to wick into the composite.
- The degradation of the outer most layers due to acid exposure facilitated the transfer of the stress caused by the applied load toward the inner core region of the cross-section, thus creating helical cracks on the surface of glass fibers in that region.
- The existence of the perforation in the composite pipes proved to have more significant influence on the load carrying capacity and axial stiffness of the pipes in comparison to the effect of aging. However, in order to reach to a more decisive conclusion on this observation, longer length perforated pipes should be fabricated, aged, and tested, so to further establish the influence of the ratio of the exposed surface area to the perforation cross-section area on the overall degradation of perforated aged composites.

Acknowledgments

The financial support of the Natural Sciences and Engineering Research Council of Canada is gratefully acknowledged. The assistance of Dr. Taheri Behrooz in fabricating the pipes is gratefully acknowledged.

References

[1] Perreux D, Suri C. A study of the coupling between the phenomena of water absorption and damage in glass epoxy composite pipes. Compos. Sci. Technol. 1997;57:1403–1413.
[2] Bunsell AR. Hygrothermal ageing of composite materials. In: Proc. Compos. Mater. Petrol. Indust.; 1994; Rueil-Malmaison.
[3] Aveston J, Kelly J, Sillwood JM. Long term strength of glass reinforced plastics in wet environments. In: Proc. 3rd Conf. Compos. Mater.; 1980; Oxford. p. 556–568.
[4] Startsev OV, Krotov AS, Startseva LT. Interlayer shear strength of polymer composite materials during long term climatic ageing. Polym. Degrad. Stab. 1999;63:183–186.
[5] Tsotsis TK, Keller S, Lee K, Bardis J, Bish J. Aging of polymeric composite specimens for 5000 hours at elevated pressure and temperature. Compos. Sci. Technol. 2001;61:75–86.
[6] Boukhoulda FB, Guillaumat L, Lataillade JL, Adda-Bedia E, Lousdad A. Aging-impact coupling based analysis upon glass/polyester composite material in hygrothermal environment. Mater. Des. 2011;32:4080–4087.
[7] Liao K, Schultheisz CR, Hunston DL. Effects of environmental aging on the properties of pultruded GFRP. Composites Part B. 1999;30:485–493.

[8] Abdel-Magid B, Ziaee S, Gass K, Schneider M. The combined effects of load, moisture and temperature on the properties of E-glass/epoxy composites. Compos. Struct. 2005;71:320–326.
[9] Bagherpour S, Bagheri R, Saatchi A. Effects of concentrated HCl on the mechanical properties of storage aged fiber glass polyester composite. Mater. Des. 2009;30:271–274.
[10] Ellyin F, Maser R. Environmental effects on the mechanical properties of glass-fiber epoxy composite tubular specimens. Compos. Sci. Technol. 2004;64:1863–1874.
[11] Guedes RM, Sa A, Faria H. Influence of moisture absorption on creep of GRP composite pipes. Polym. Test. 2007;26:595–605.
[12] Yao J, Ziegmann G. Equivalence of moisture and temperature in accelerated test method and its application in prediction of long-term properties of glass-fiber reinforced epoxy pipe specimen. Polym. Test. 2006;25:149–157.
[13] d'Almedia JRM, de Almedia RC, de Lima WR. Effect of water absorption of the mechanical behavior of fiberglass pipes used for offshore service waters. Compos. Struct. 2008;83:221–225.
[14] Maxwell AS, Broughton WR, Dean G, Sims GD. Review of accelerated aging methods and lifetime prediction techniques for polymeric materials. NLP Report, DEPC MPR 016. Teddington (UK): National Physical Laboratory; 2005.